Proceedings of IMECE'03
2003 ASME International Mechanical Engineering Congress
Washington, D.C., November 15–21, 2003

**IMECE2003-55283**

# A SCALE ANALYSIS APPROACH TO THERMAL CONTACT RESISTANCE

M. Bahrami[1], J. R. Culham[2], and M. M. Yovanovich[3]
Microelectronics Heat Transfer Laboratory,
Department of Mechanical Engineering,
University of Waterloo, Waterloo, Canada N2L 3G1

## ABSTRACT

A new analytical model is developed for predicting thermal contact resistance (TCR) of non-conforming rough contacts of bare solids in a vacuum. Instead of using probability relationships to model the size and number of microcontacts of Gaussian surfaces, a novel approach by employing the "scale analysis methods" is taken. It is shown that the mean size of the microcontacts is proportional to the surface roughness and inversely proportional to the surface asperity slope. A general relationship for determining TCR is derived by superposition of the macro and the effective micro thermal resistances. The present model allows TCR to be predicted over the entire range of non-conforming rough contacts from conforming rough to smooth Hertzian contacts. It is demonstrated that the geometry of heat sources on a half-space for microcontacts is justifiable and that the effective micro thermal resistance is not a function of surface curvature. A comparison of the present model with 604 experimental data points, collected by many researchers during the last forty years, shows good agreement for the entire range of TCR. The data covers a wide range of materials, mechanical and thermophysical properties, micro and macro contact geometries, and similar and dissimilar metal contacts.

## Nomenclature

| | | |
|---|---|---|
| $A$ | = | area, $m^2$ |
| $a$ | = | radius of contact, $m$ |
| $b$ | = | flux tube radius, $m$ |
| $c$ | = | scale analysis constant |
| $c_1, c_2$ | = | Vickers microhardness coefficients, $GPa$, $-$ |
| CS | = | carbon steel |
| $d_v$ | = | Vickers indentation diagonal, $\mu m$ |
| $dr$ | = | increment in radial direction, $m$ |
| $E$ | = | Young's modulus, $GPa$ |
| $E'$ | = | effective elastic modulus, $GPa$ |
| $F$ | = | external force, $N$ |
| $h$ | = | contact conductance, $W/m^2K$ |
| $H_{mic}$ | = | microhardness, $GPa$ |
| $H'$ | = | $c_1 (\sigma'/m)^{c_2}$, $GPa$ |
| $k$ | = | thermal conductivity, $W/mK$ |
| $L$ | = | length scale $\equiv b_L^2 / (\sigma/m)$, $m$ |
| $m$ | = | effective mean absolute surface slope |
| $n_s$ | = | number of microcontacts |
| $P$ | = | pressure, $Pa$ |
| $P^*$ | = | non-dimensional pressure $\equiv F/\left(\pi H' b_L^2\right)$ |
| $Q$ | = | heat flow rate, $W$ |
| $R$ | = | thermal resistance, $K/W$ |
| $R^*$ | = | non-dimensional thermal resistance |
| $T$ | = | temperature, $K$ |
| $Y$ | = | mean surface plane separation, $m$ |

*Greek*

| | | |
|---|---|---|
| $\alpha$ | = | non-dimensional parameter $\equiv \sigma\rho/a_H^2$ |
| $\delta$ | = | max surface out-of-flatness, $m$ |
| $\varepsilon$ | = | flux tube relative radius, $a/b$ |
| $\theta$ | = | angle of the surface asperities, $rad$ |
| $\psi$ | = | spreading resistance factor |
| $\rho$ | = | radius of curvature, $m$ |
| $\sigma$ | = | RMS surface roughness, $\mu m$ |
| $\sigma_0$ | = | roughness reference value $=1$ $\mu m$ |
| $\tau$ | = | non-dimensional parameter $\equiv \rho/a_H$ |
| $\upsilon$ | = | Poisson's ratio, $-$ |

[1]Ph.D. Candidate, Department of Mechanical Engineering.
[2]Associate Professor, Director, Microelectronics Heat Transfer Laboratory. Member ASME .
[3]Distinguished Professor Emeritus, Department of Mechanical Engineering. Fellow ASME.

*Subscripts*

| | | |
|---|---|---|
| 0 | = | value at origin |
| 1, 2 | = | surface 1,2 |
| $a$ | = | apparent |
| $EC$ | = | elastoconstriction |
| $H$ | = | Hertz |
| $j$ | = | joint |
| $L$ | = | large |
| $mic$ | = | microcontact |
| $P$ | = | plastic deformation |
| $r$ | = | real |
| $s$ | = | small, solids |
| $v$ | = | Vickers |

## 1 INTRODUCTION

Heat transfer through interfaces formed by mechanical contact of rough solids has many important applications such as in microelectronics chip cooling, spacecraft structures, and nuclear fuel temperature prediction.

Heat transfer across the interface can take place by three different modes, i) conduction at the microcontacts, ii) conduction through the interstitial fluid in the gap between the contacting solids, and iii) thermal radiation across the gap. The radiation heat transfer remains small and can be neglected for surface temperatures up to 700 $K$ [1]. Since in this study the interstitial fluid is assumed to be absent, the only remaining heat transfer mode is conduction through the microcontacts.

Engineering or real surfaces have roughness and surface curvature/out-of-flatness simultaneously. Due to surface roughness, contact between two surfaces occurs only over microscopic contacts which are located in the "contact plane". The real area of contact, i.e., the total area of microcontacts, is a small fraction of the nominal contact area, typically a few percent [2, 3]. As illustrated in Fig. 1, the macrocontact area, the area where microcontacts are distributed, is formed as a result of surface curvature of contacting bodies. Heat flow is constricted to pass through the macrocontact and then microcontacts. This phenomenon is observed through a relatively high temperature drop across the interface. Here an example is given to show the magnitude and relative importance of TCR versus the "bulk resistance". Consider a 3 $cm^2$ flat SS plate with the thickness of 5 $mm$ which has a surface roughness of 1 $\mu m$. The TCR for the bare joint in a vacuum with 0.1 $MPa$ contact pressure, is in the order of 30 $K/W$ as compared to the plate bulk resistance of 0.2 $K/W$.

Categorizing TCR modeling procedures into geometrical, mechanical and thermal analyses, Bahrami et al. [4] reviewed the existing theoretical TCR models and discussed aspects of each component of the analysis in detail.

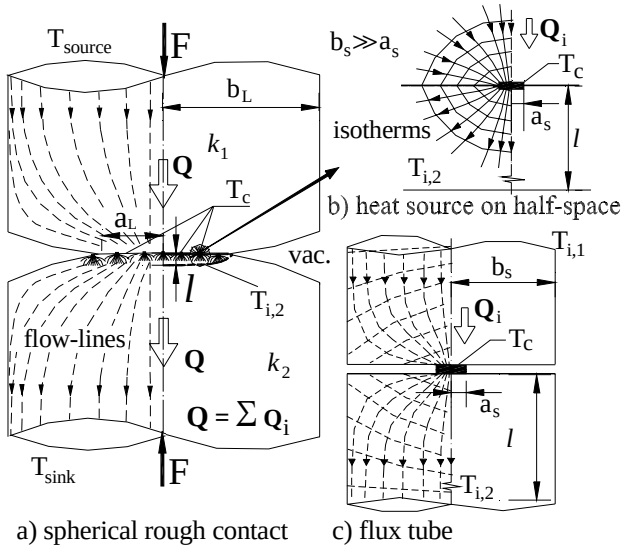


Figure 1. GEOMETRY OF SPHERICAL ROUGH CONTACT IN VACUUM, HEAT SOURCE ON HALF-SPACE, AND FLUX TUBE GEOMETERIES

Comparing with more than 400 experimental data points, Bahrami et al.[1] showed that the existing analytical models are applicable only to the limiting cases namely conforming rough contacts and smooth sphere-flat contacts and do not cover the entire range of TCR. Therefore, the need for a theoretical model that can predict TCR over the entire range of contacts still exists.

The objective of this study is to develop a compact analytical model for predicting TCR for the entire range of non-conforming rough contacts, i.e., from conforming rough to smooth sphere-flat contact. A novel approach is taken by employing scale analysis methods to achieve this goal.

## 2 THEORETICAL BACKGROUND

Analytical, experimental and numerical models have been developed to predict thermal contact resistance (TCR) since the 1930's. A large number of publications on TCR exist in the literature, to name a few Clausing and Chao [5], Lambert and Fletcher [6], and Nishino et al. [7] can be mentioned, which indicates that the development of a general predictive model is a difficult task. A comprehensive review of literature can be found in Bahrami et al. [4]. Here only a short review of the materials used to develop the present model is given.

According to the examination of the microgeometry of rough surfaces, surface asperities have small slopes and curved shapes at their summits [8, 9]. It is a common

methodology to simplify the contact of two Gaussian rough surfaces by the contact of a smooth plane with a random rough surface which has equivalent surface characteristics. The equivalent surface roughness $\sigma$ and surface slope $m$ can be found from

$$\sigma = \sqrt{\sigma_1^2 + \sigma_2^2} \quad \text{and} \quad m = \sqrt{m_1^2 + m_2^2} \tag{1}$$

Cooper et al. [10] proved that the microcontacts can be assumed isothermal provided the thermal conductivity in each body is independent of direction, position and temperature.

Thermal spreading resistance is defined as the difference between the average temperature of the contact area and the average temperature of the heat sink/heat source, divided by the total heat flow rate $Q$ [11], i.e., $R = \Delta T/Q$. The real shapes of microcontacts can be a wide variety of singly connected areas depending on the local profile of the contacting asperities. Yovanovich et al. [12] studied the steady-state thermal constriction resistance of a singly connected planar contact of arbitrary shape. They proposed a definition for thermal constriction resistance based on the square root of the contact area. The square root of contact area was found to be the characteristic dimension and a non-dimensional constriction resistance based on the square root of area was proposed, which varied by less than 5% for all shapes considered. Therefore, the real shape of the microcontacts would be a second order effect and an equivalent circular contact, which has the same area, can represent the microcontacts.

Yovanovich and Hegazy [13] showed through experiments that the surface microhardness is much higher than the bulk hardness and that the microhardness decreases as the indentation depth increases until the bulk hardness is reached. They proposed a correlation for determining the microhardness, $H_{\mathsf{mic}} = c_1 \left(d_{\mathsf{v}}/\sigma_0\right)^{c_2}$, where $d_{\mathsf{v}}\,(\mu m)$, $c_1\,(GPa)$, $c_2\,(-)$, and $\sigma_0 = 1\,(\mu m)$ are the Vickers indentation diagonal, correlation coefficients determined from the Vickers microhardness measurement, and a reference value, respectively. Microhardness depends on several parameters: mean surface roughness, mean absolute slope of asperities, method of surface preparation, and applied pressure. Sridhar and Yovanovich [14] suggested empirical relations to estimate Vickers microhardness coefficients, using the bulk hardness of the material. Two least-square-cubic fit expressions were reported

$$\begin{aligned} c_1 &= H_{\mathsf{BGM}} \left(4.0 - 5.77\kappa + 4.0\kappa^2 - 0.61\kappa^3\right) \\ c_2 &= -0.57 + 0.82\kappa - 0.41\kappa^2 + 0.06\kappa^3 \end{aligned} \tag{2}$$

where $\kappa = H_{\mathsf{B}}/H_{\mathsf{BGM}}$, $H_{\mathsf{B}}$ is the Brinell hardness of the bulk material, and $H_{\mathsf{BGM}} = 3.178(GPa)$. The above correlations are valid for the range $1.3 \leq H_{\mathsf{B}} \leq 7.6\ (GPa)$, the RMS percent difference between data and calculated values were reported; 5.3% and 20.8% for $c_1$, and $c_2$, respectively. Milanez et al. [15] studied the effect of microhardness coefficients on TCR by comparing the TCR's computed from the measured versus the estimated, from Eq. (2), microhardness coefficients. They concluded that despite the difference between the measured and estimated values of microhardness coefficients, the TCR's predicted by both methods are in good agreement.

As shown in Fig. 1, there are two geometries that can be used as basic elements to model the thermal constriction/spreading resistance of the microcontacts, i) heat source on half-space in which microcontacts are (assumed to be) located far from each other, where thermal constriction/spreading resistance can be found [11]

$$R_{\mathsf{mic,\ half\text{-}space}} = \frac{1}{2k_{\mathsf{s}}a_{\mathsf{s}}} \tag{3}$$

ii) the flux tube geometry, considering the effect of neighboring microcontacts. Cooper et al. [10] proposed a simple accurate correlation for determining the flux tube constriction/spreading resistance,

$$R_{\mathsf{mic,\ flux\ tube}} = \frac{\psi\left(\varepsilon_{\mathsf{s}}\right)}{2k_{\mathsf{s}}a_{\mathsf{s}}} \tag{4}$$

where $\psi\left(\varepsilon_{\mathsf{s}}\right) = \left(1 - \varepsilon_{\mathsf{s}}\right)^{1.5}$ and $\varepsilon_{\mathsf{s}} = a_{\mathsf{s}}/b_{\mathsf{s}}$.In Eq. (4), it is assumed that the radii of two contacting bodies are the same, i.e., $b_1 = b_2 = b$. In general case where $b_1 \neq b_2$, thermal spreading resistance will be, $R_{\mathsf{flux\ tube}} = \psi\left(a/b\right)/4ka$.

In the case of smooth spherical contact, the Hertzian theory can be used to calculate the radius of the macrocontact area, $a_{\mathsf{Hz}}$. Hertz replaced the geometry of two spheres by a flat surface and an equivalent sphere, where the effective radius of curvature is, $1/\rho = 1/\rho_1 + 1/\rho_2$. Hertz derived a relationship for the radius of the contact area

$$\begin{aligned} a_{\mathsf{H}} &= \left(\frac{3F\rho}{4E'}\right)^{1/3} \\ \frac{1}{E'} &= \frac{1 - \upsilon_1^2}{E_1} + \frac{1 - \upsilon_2^2}{E_2} \end{aligned} \tag{5}$$

where $E$, $\upsilon$, and $E'$ are the Young's modulus, Poisson's ratio, and the effective elastic modulus, respectively. Clausing and Chao [5] modeled the surface out-of-flatness by a spherical profile. The relationship between the equivalent radius

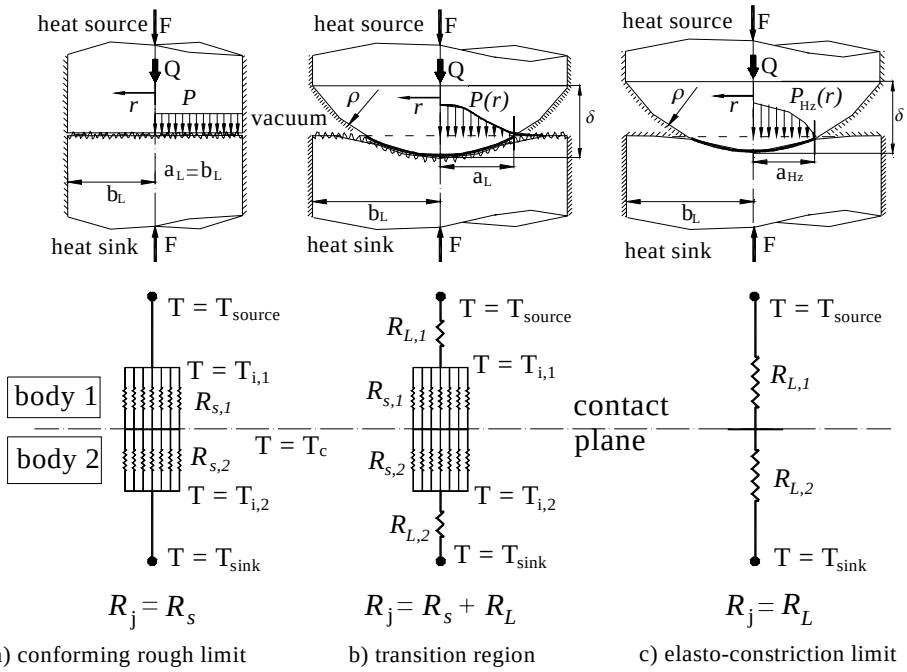


Figure 2. GEOMETRY AND THERMAL RESISTANCE NETWORK: CONFORMING ROUGH, ELASTO-CONSTRICTION, AND TRANSITION REGIONS

of curvature and the surface out-of-flatness is $\rho = b_{\mathsf{L}}^2/2\delta$, where $\delta$ is the maximum out-of-flatness of the surface, see Fig. 2. Using the flux tube correlation, Eq. (4), the joint resistance for the smooth sphere-flat contact, i.e., elasto-constriction [16] limit can be determined from

$$R_{\mathsf{j,\ EC}} = \frac{(1 - a_{\mathsf{H}}/b_{\mathsf{L}})^{1.5}}{2k_{\mathsf{s}}a_{\mathsf{H}}} \tag{6}$$

Comparison between the elasto-constriction model, i.e., Eq. (6) and the smooth sphere-flat experimental data shows good agreement [4], thus the flux tube solution can be employed for determining the macro thermal resistance.

## 3 MACRO AND MICRO THERMAL RESISTANCES

As illustrated in Fig. 1, the heat flow rate $Q$ which is being transferred from the heat source at $T_{\mathsf{source}}$ to the contact plane at $T_{\mathsf{c}}$, experiences the macro thermal constriction $R_{\mathsf{L},1}$, which arose due to the macrocontact area. Heat is then passed through $n_{\mathsf{s}}$ (parallel) microcontacts in the contact plane, which is called the microcontact resistance, $R_{\mathsf{s}}$.

Assuming circular isothermal microcontacts, at $T_{\mathsf{c}}$, that have the mean radius (in the order of $a_{\mathsf{s}} \sim \mu m$), isothermal planes must exist at intermediate temperatures $T_{\mathsf{i},1}$ and $T_{\mathsf{i},2}$, i.e., $T_{\mathsf{source}} < T_{\mathsf{i},1} < T_{\mathsf{c}} < T_{\mathsf{i},2} < T_{\mathsf{sink}}$ at some location $l$ above/below the contact plane in body 1 and 2, respectively. If the microcontacts are considered as heat sources on half-space the distance between these intermediate isothermal planes and the contact plane $l = 40a_{\mathsf{s}} \sim 40\ \mu m$ [11]. As microcontacts grow in size and number they start to effect each other (the flux tube geometry) and $l$ decreases, $l \sim b_{\mathsf{s}}$ [17]. Consequently, macro thermal constriction/spreading resistances $R_{\mathsf{L},1}$ and $R_{\mathsf{L},2}$ are in series between the heat source and the isothermal plane $T_{\mathsf{i},1}$ and the isothermal plane $T_{\mathsf{i},2}$ and the heat sink, respectively. Therefore, TCR of a non-conforming rough joint in a vacuum can be written as

$$R_{\mathsf{j}} = R_{\mathsf{L}} + R_{\mathsf{s}} \tag{7}$$

where $R_{\mathsf{L}} = R_{\mathsf{L},1} + R_{\mathsf{L},2}$, $R_{\mathsf{s}} = R_{\mathsf{s},1} + R_{\mathsf{s},2}$, and

$$\frac{1}{R_{\mathsf{s,\ 1\ or\ 2}}} = \sum^{n_{\mathsf{s}}} \frac{1}{R_{\mathsf{mic,\ 1\ or\ 2}}}$$

where $R_{\mathsf{mic,\ 1\ or\ 2}}$ is the thermal constriction/spreading resistance of a single microcontact in body 1 or 2.

Equation (7) is a general expression and applicable to all spherical rough contacts. Two limiting cases can be distinguished for Eq. (7), i) the conforming rough limit, i.e.,

contact of flat rough surfaces where the surface curvatures are very large thus macro thermal resistance $R_{\mathsf{L}}$ is negligible and micro thermal resistance $R_{\mathsf{s}}$ is the controlling part, ii) the elastoconstriction limit where the radii of curvature of contacting bodies are small and surfaces are smooth, thus the macro thermal resistance $R_{\mathsf{L}}$ is predominant and $R_{\mathsf{s}}$ is negligible, and iii) transition region or general contact in which both $R_{\mathsf{L}}$ and $R_{\mathsf{s}}$ exist and have the same order of magnitude. Figure 2 shows the above-mentioned regions and their corresponding thermal resistance networks.

## 4 THE PRESENT MODEL

Due to the random nature of surface roughness studying the deformation and heat transfer of each single asperity is impossible, instead a representative (modeled) asperity is chosen and studied. Surface roughness is modeled by assuming Gaussian distribution of asperities. The RMS surface roughness $\sigma$ is a representative for the mean surface asperity heights.

In this section, using scale analysis, first an expression is derived for TCR of conforming rough contacts, $R_{\mathsf{s}}$. Then, the non-conforming macrocontact area is divided into infinitesimal surface elements where the conforming rough model relation can be applied. By integrating the local microcontact resistance over the macrocontact, an effective microcontacts resistance $R_{\mathsf{s}}$ is found. Using the flux tube correlation, the macrocontact resistance $R_{\mathsf{L}}$ is computed. Finally, superimposing the macro and micro thermal resistances, Eq. (7), the joint resistance is determined.

### 4.1 Conforming Rough Contact Limit

Surface roughness can be visualized as shallow valleys and hills with small slopes where asperities have spherical shapes at their summits. Figure 3 illustrates a model asperity, which represents the equivalent rough surface characteristics $\sigma$ and $m$, placed in contact with a smooth plate at the mean separation $Y$. Using the equivalent rough surface simplification and considering the fact that the mean surface slope, $m$, is small, the microcontacts are circular, flat and all in the same contact plane. Figure 3 also illustrates proportionalities between the mean microcontact radius $a_{\mathsf{s}}$ and the surface roughness $\sigma$ and slope $m$. As surface slope slightly decreases from $m$ to $m-\delta m$, while the roughness $\sigma$ and $Y$ are held constant, the mean radius of microcontacts increases and visa versa, thus one can write $a_{\mathsf{s}} \sim 1/m$. Following the same method for surface roughness, we obtain $a_{\mathsf{s}} \sim \sigma$. Combining the above proportionalities, the mean radius of the microcontacts is proportional to the surface roughness and inversely proportional to the surface slope,

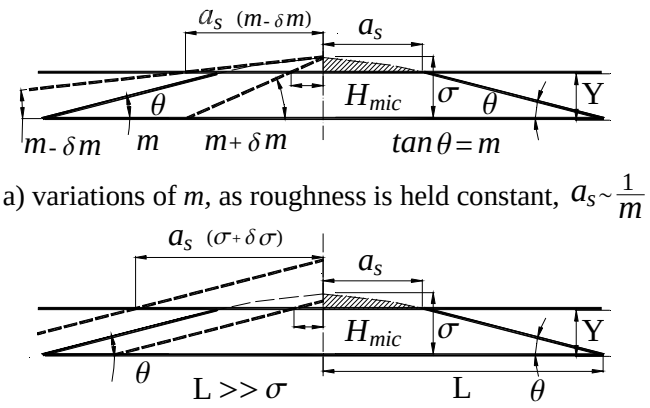


Figure 3. PROPORTIONALITIES BETWEEN MICROCONTACT SIZE AND SURFACE SLOPE AND ROUGHNESS

i.e.,

$$a_{\mathsf{s}} \sim \frac{\sigma}{m} \tag{8}$$

Considering $n_{\mathsf{s}}$ circular microcontacts with the mean radius of $a_{\mathsf{s}}$ within the contact area, the real contact area is

$$A_{\mathsf{r}} = \pi n_{\mathsf{s}} a_{\mathsf{s}}^2 \sim \pi n_{\mathsf{s}} \left(\frac{\sigma}{m}\right)^2 \tag{9}$$

The microcontacts are assumed to deform plastically. In other words, each microcontact can be visualized as a small microhardness indentation. The empirical correlation proposed by Yovanovich and Hegazy [13], see section 2, is used to estimate the microhardness. Preserving the microcontact area, i.e., $A_{\mathsf{v}} = \pi a_{\mathsf{s}}^2$, where $A_{\mathsf{v}}$ is the projected area of the Vickers microhardness test, the Vickers indentation diagonal $d_{\mathsf{v}}$ can be related to the mean radius of microcontacts $a_{\mathsf{s}}$, $d_{\mathsf{v}} = \sqrt{2\pi} a_{\mathsf{s}}$, microhardness becomes,

$$H_{\mathsf{mic}} \sim H' \equiv c_1 \left(\frac{\sigma}{m\sigma_0}\right)^{c_2} \tag{10}$$

Assuming plastic deformation of microcontacts, external force can be related to the real contact area and surface microhardness through a force balance:

$$F = A_{\mathsf{r}} H_{\mathsf{mic}} \sim \pi n_{\mathsf{s}} \left(\frac{\sigma}{m}\right)^2 H' \tag{11}$$

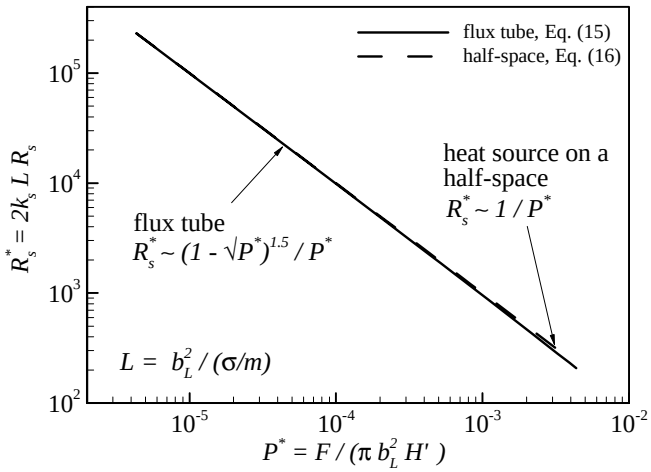


Figure 4. COMPARISON BETWEEN HALF-SPACE AND FLUX TUBE SOLUTIONS

where $H_{\mathsf{mic}}$ is the microhardness of the softer material in contact. From Eq. (11) the number of microcontacts can be determined

$$n_{\mathsf{s}} \sim \frac{F}{\pi \left(\sigma/m\right)^2 H'} \tag{12}$$

It can be seen from Eq. (12) that an increase in load creates new microcontacts while the mean size of microcontacts remain constant, i.e., $a_{\mathsf{s}} \sim \sigma/m$. This is in agreement with Greenwood and Williamson [3] and also satisfies the proportionality $A_{\mathsf{r}} \sim F$ reported by Tabor [2].

The thermal model is based on the premise that $n_{\mathsf{s}}$ heat channels, covering the nominal contact area, form a set of parallel paths for transferring heat flow. If the half-space assumption is considered, see Fig. 1-b, TCR can be found from,

$$R_{\mathsf{s,\ half\text{-}space}} = \frac{1}{2k_{\mathsf{s}} n_{\mathsf{s}} a_{\mathsf{s}}} \sim \frac{1}{2k_{\mathsf{s}} n_{\mathsf{s}} \left(\sigma/m\right)} \tag{13}$$

Many researchers including Cooper et al. [10] modeled the micro thermal constriction/spreading resistance using the flux tube geometry. In this case TCR is,

$$R_{\mathsf{s,\ flux\ tube}} = \frac{\psi\left(\varepsilon_{\mathsf{s}}\right)}{2k_{\mathsf{s}} n_{\mathsf{s}} a_{\mathsf{s}}} \sim \frac{\psi\left(\varepsilon_{\mathsf{s}}\right)}{2k_{\mathsf{s}} n_{\mathsf{s}} \left(\sigma/m\right)} \tag{14}$$

where $\psi\left(\cdot\right)$ is the constriction alleviation factor given in Eq. (4). The apparent contact area is covered by flux tubes with the mean radius $b_{\mathsf{s}}$, the relative size of microcontacts can be found from, $\varepsilon_{\mathsf{s}} = a_{\mathsf{s}}/b_{\mathsf{s}} = \sqrt{A_{\mathsf{r}}/A_{\mathsf{a}}}$, where $A_{\mathsf{a}} = \pi b_{\mathsf{L}}^2$. Substituting $A_{\mathsf{r}}$ and $A_{\mathsf{a}}$ one obtains

$$\varepsilon_{\mathsf{s}} \sim \sqrt{\frac{F/\pi b_{\mathsf{L}}^2}{H'}} \equiv \sqrt{P^*} \tag{15}$$

where $P^*$ is a non-dimensional parameter that can be interpreted as the ratio of contact pressure to the pressure at the microcontacts. Re-arranging Eq. (12), the number of microcontacts can be expressed in terms of $P^*$,

$$n_{\mathsf{s}} \sim \frac{b_{\mathsf{L}}^2}{\left(\sigma/m\right)^2} P^* \tag{16}$$

Using the non-dimensional parameter $P^*$, the TCR for conforming rough surfaces, using the flux tube solution, can be re-written as

$$R_{\mathsf{s,\ flux\ tube}} \sim \frac{\left(\sigma/m\right)\left(1-\sqrt{P^*}\right)^{1.5}}{2k_{\mathsf{s}}\ b_{\mathsf{L}}^2\ P^*} \tag{17}$$

or in the non-dimensional form

$$R^*_{\mathsf{s,\ flux\ tube}} = 2k_{\mathsf{s}} L R_{\mathsf{s}} \sim \frac{\left(1-\sqrt{P^*}\right)^{1.5}}{P^*} \tag{18}$$

where $L = b_{\mathsf{L}}^2/\left(\sigma/m\right)$ is the conforming rough limit length scale. Substituting Eq. (16) in Eq. (13) the TCR for conforming rough surfaces, using the heat source on half-space solution, can be written as

$$R^*_{\mathsf{s,\ half\text{-}space}} \sim \frac{1}{P^*} \tag{19}$$

Figure 4 shows the comparison between Eqs. (18) and (19). It can be seen that over a wide range of $P^*$ they are almost identical and show very good agreement. However, as expected, at relatively large values of $P^*$ the half-space relationship, Eq. (19), shows slightly higher resistances than the flux tube. The RMS relative difference between two relationships is less than 4 percent. Therefore, the microcontacts can be modeled as heat sources on half-space and Eq. (19) is chosen for thermal analysis of microcontacts.

Using these powerful scale analysis techniques, Eq. (19) was derived which illustrates that the TCR of microcontacts is inversely proportional to the dimensionless pressure (or

external load). To find the equality or exact relationship, Eq. (19) must be multiplied by the scale analysis constant, $c$, which can be found through comparison with experimental data, i.e.,

$$R_{\mathsf{s}}^{*} = \frac{c}{P^{*}} \tag{20}$$

The dimensional forms of thermal resistance and conductance using $h_{\mathsf{s}} = 1/\left(R_{\mathsf{s}} A_{\mathsf{a}}\right)$, are

$$\begin{aligned} R_{\mathsf{s}} &= \frac{\pi c \left(\sigma/m\right) H'}{2 k_{\mathsf{s}} F} \\ h_{\mathsf{s}} &= \frac{2}{\pi c} k_{\mathsf{s}} \left(\frac{m}{\sigma}\right) \frac{P}{H'} \end{aligned} \tag{21}$$

where $c$ and $P = F/\left(\pi b_{\mathsf{L}}^{2}\right)$ are the scale analysis constant, and the nominal pressure, respectively.

Experimental data collected by Antonetti [18], Hegazy [19], and Milanez et al. [20] are non-dimensionalized and plotted along with Eq. (20) in Fig. 5. The constant of the scale analysis $c$, Eq. (20), was found to be $c = 0.36$, which minimizes the RMS difference between the model and the experimental data. Figure 5 illustrates the comparison between the scale analysis relationship and the data. The RMS relative difference between the data and the relationship is about 12% over the entire range of the comparison. Table 1 indicates the researchers and the specimen materials used in the experiments.

### 4.2 General Model

Bahrami et al. [21] studied mechanical contact of spherical rough surfaces. Assuming elastic bulk deformation and plastic deformation for microcontacts, a general contact pressure distribution was proposed which covers all possible contacts ranging from the spherical rough to the Hertzian contact. They proposed a simple correlation for calculating the radius of the macrocontact as a function of two non-dimensional parameters,

$$a_{\mathsf{L}} = 1.80\ a_{\mathsf{H}}\ \frac{\sqrt{\alpha + 0.31\tau^{0.056}}}{\tau^{0.028}} \tag{22}$$

where $\alpha = \sigma\rho/a_{\mathsf{H}}^{2}$ and $\tau = \rho/a_{\mathsf{H}}$ are the roughness parameter introduced by Johnson [8] and the geometric parameter, respectively.

Using the flux tube correlation, Eq. (4), and the radius of the macrocontact area given by Eq. (22), thermal macro

Table 1. RESEARCHERS AND SPECIMEN MATERIALS USED IN COMPARISONS

| Ref. | Researcher | Material(s) |
|---|---|---|
| A | Antonetti [18] | Ni200<br>Ni200-Ag |
| B | Burde [22] | SPS 245, CS |
| CC | Clausing-Chao [23] | Brass Anaconda<br>Mg AZ 31B<br>SS303 |
| F | Fisher [24] | Ni 200-Carbon Steel |
| H | Hegazy [19] | Ni200<br>SS304<br>Zircaloy4<br>Zr-2.5%wt Nb |
| K | Kitscha [25] | Steel 1020-CS |
| MM | McMillan-Mikic [26] | SS303 |
| MR | Mikic-Rohsenow [17] | SS305 |
| M | Milanez et al. [20] | SS304 |

resistance can be calculated from

$$R_{\mathsf{L}} = \frac{\left(1 - a_{\mathsf{L}}/b_{\mathsf{L}}\right)^{1.5}}{2 k_{\mathsf{s}} a_{\mathsf{L}}} \tag{23}$$

The macrocontact area is a circle, thus the heat transferred in a non-conforming rough contact under vacuum conditions can be calculated from,

$$Q = 2\pi \Delta T_{\mathsf{s}} \int_{0}^{a_{\mathsf{L}}} h_{\mathsf{s}}\left(r\right) r dr \tag{24}$$

where $h_{\mathsf{s}}\left(r\right)$, $\Delta T_{\mathsf{s}} = T_{\mathsf{i},1} - T_{\mathsf{i},2}$ are the local thermal conductance, and the effective temperature difference for microcontacts, respectively. The effective micro thermal conductance for a joint can be defined as $h_{\mathsf{s}} = Q/\left(A_{\mathsf{a}} \Delta T_{\mathsf{s}}\right)$. Therefore, the effective microcontact conductance is

$$h_{\mathsf{s}} = \frac{2\pi}{A_{\mathsf{a}}} \int_{0}^{a_{\mathsf{L}}} h_{\mathsf{s}}\left(r\right) r dr \tag{25}$$

or in terms of thermal resistance, where $R = 1/\left(h A_{\mathsf{a}}\right)$,

$$R_{\mathsf{s}} = \frac{1}{2\pi} \left[\int_{0}^{a_{\mathsf{L}}} h_{\mathsf{s}}\left(r\right) r dr\right]^{-1} \tag{26}$$

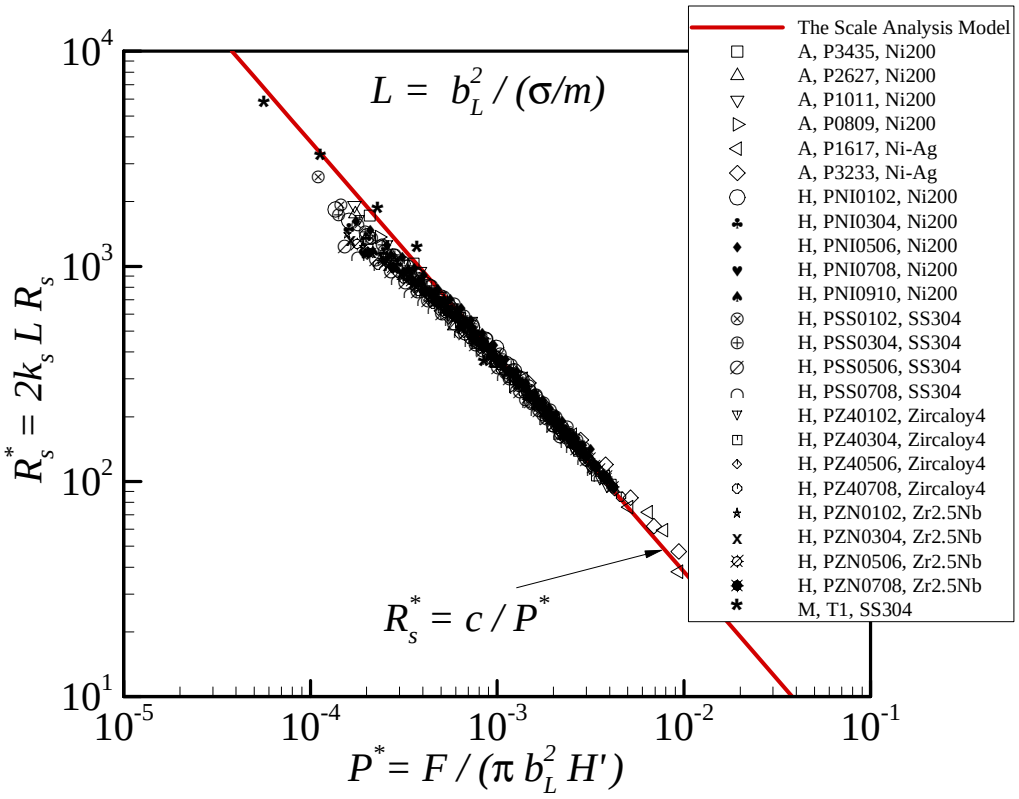


Figure 5. COMPARISON OF SCALE ANALYSIS RELATIONSHIP WITH DATA AT CONFORMING ROUGH LIMIT

Assuming constant pressure in surface elements $dr$, the local thermal conductance at $r$ can be calculated from Eq. (21),

$$h_{\mathrm{s}}(r) = \frac{2}{c\pi} k_{\mathrm{s}} \left(\frac{m}{\sigma}\right) \frac{P(r)}{H'} \tag{27}$$

where $P(r)$ is the local contact pressure at $r$. Substituting Eq. (27) into Eq. (26), one obtains

$$R_{\mathrm{s}} = \frac{cH'(\sigma/m)}{4k_{\mathrm{s}}} \left[\int_0^{a_{\mathrm{L}}} P(r)\, r dr\right]^{-1} \tag{28}$$

From a force balance, we know that $F = 2\pi \int_0^{a_{\mathrm{L}}} P(r)\, r dr$, therefore Eq. (28) simplifies to

$$R_{\mathrm{s}} = \frac{c\pi H'(\sigma/m)}{2k_{\mathrm{s}} F} \tag{29}$$

Equations (21) and (29) are identical also the effective thermal micro resistance $R_{\mathrm{s}}$ is not a function of the surface curvature. Additionally, the pressure distribution profile does not affect the thermal micro resistance. The micro thermal resistance $R_{\mathrm{s}}$ is independent of the surface curvature, however it can be observed through experiments that the joint resistance $R_{\mathrm{j}}$ increases as surface curvature decreases from the conforming ($\rho \to \infty$) to non-conforming contacts. As the surface curvature decreases the macrocontact area and consequently the macro resistance $R_{\mathrm{L}}$ are formed, but $R_{\mathrm{s}}$ remains unchanged as surface curvature varies, Eq. (29).

By superimposing the macro and the micro resistances, Eq. (7), thermal joint resistance for the general contact case is obtained

$$R_{\mathrm{j}} = \frac{0.36\pi H'(\sigma/m)}{2k_{\mathrm{s}} F} + \frac{(1 - a_{\mathrm{L}}/b_{\mathrm{L}})^{1.5}}{2k_{\mathrm{s}} a_{\mathrm{L}}} \tag{30}$$

Equation (30) is a general relationship that covers both limiting cases. It can be easily seen that in the conforming rough limit, where $a_{\mathrm{L}} \to b_{\mathrm{L}}$ the macro resistance $R_{\mathrm{L}} \to 0$, Eq. (21). Also, in the elastoconstriction limit, where $\sigma \to 0$ the micro resistance $R_{\mathrm{s}} \to 0$ and $a_{\mathrm{L}} \to a_{\mathrm{H}}$ and Eq. (30) yields Eq. (6).

The assumptions of the present model can be summarized as follows

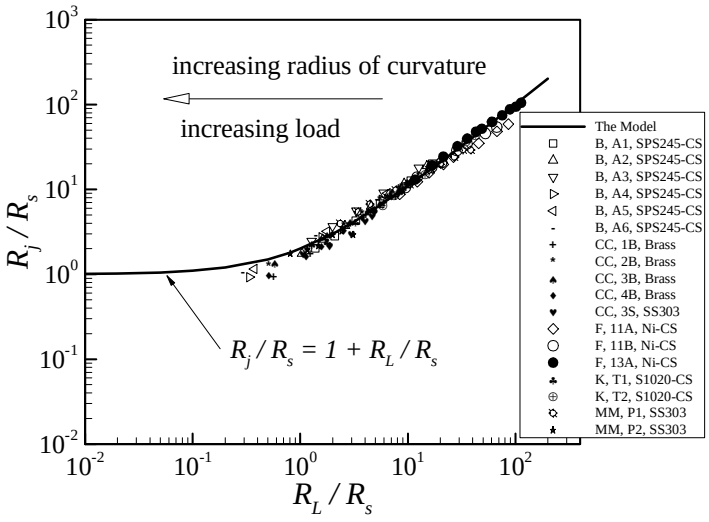


Figure 6. COMPARISON OF GENERAL MODEL WITH NON-CONFORMING ROUGH DATA

- contacting solids are randomly rough, isotropic
- surfaces are clean
- contacting solids are thick relative to surface roughness
- contact is static
- contact occurs in a vacuum
- radiation heat transfer is negligible
- microcontacts are circular and isothermal
- only the first-time contact is considered
- steady-state heat transfer at microcontacts
- microcontacts deform plastically
- spherical surface out-of-flatness
- axisymmetric loading
- the bulk material deformation is elastic.

## 5 COMPARISON WITH EXPERIMENTAL DATA

Dividing both sides of Eq. (30) by $R_{\mathsf{s}}$, one obtains

$$\frac{2k_{\mathsf{s}}F}{\pi cH'\left(\sigma/m\right)}R_{\mathsf{j}} = 1 + \frac{F\left(1-a_{\mathsf{L}}/b_{\mathsf{L}}\right)^{1.5}}{\pi cH'\left(\sigma/m\right)a_{\mathsf{L}}} \qquad (31)$$

Experimental data collected by Burde [22], Clausing and Chao [23], Fisher [24], Kitscha [25], and McMillan and Mikic [26] are non-dimensionalized and compared with the model, Eq. (31), in Fig. 6. Table 1 lists the researchers and the specimen materials used in the experiments. As illustrated in Fig. 6, an increase in the external load or the radius of curvature increases the macrocontact radius $a_{\mathsf{L}}$, thus macro thermal resistance $R_{\mathsf{L}}$ decreases which results in a decrease in the joint resistance.

Equation (30) can be non-dimensionalized with respect to the conforming rough limit length scale $L$ and re-written,

$$R^*_{\mathsf{j}} = 2k_{\mathsf{s}}LR_{\mathsf{j}} = \frac{0.36}{P^*} + \frac{L\left(1-a_{\mathsf{L}}/b_{\mathsf{L}}\right)^{1.5}}{a_{\mathsf{L}}} \qquad (32)$$

where $L = b_{\mathsf{L}}^2/\left(\sigma/m\right)$ and $P^* = F/\left(\pi b_{\mathsf{L}}^2 H'\right)$.

About 600 experimental data points are non-dimensionalized and compared with the present model, Eq. (32), in Fig. 7, see Table 1 for the researchers and the specimen materials.

In most of the conforming rough data sets, such as Hegazy [19], experimental data show a lower resistance at relatively light loads compared with the model and the data approach the model as the load increases. This trend can be observed in almost all conforming rough data sets (see Fig. 7). This phenomenon which is called the *truncation effect* [20] is important at light loads when surfaces are relatively rough. A possible reason for this behavior is the Gaussian assumption of the surface asperities which implies that asperities with "infinite" heights exist. Milanez et al. [20] experimentally studied the truncation effect and proposed correlations for maximum asperities heights as functions of surface roughness.

If the external load increases beyond the elastic limit of the contacting bodies, elasto-plastic and plastic deformations occur. The plastic macrocontact radius, $a_{\mathsf{P}}$, is larger than the (elastic) radius $a_{\mathsf{L}}$, i.e., $a_{\mathsf{P}} > a_{\mathsf{L}}$. Consequently, lower TCR will be measured; this trend can be clearly seen in Fisher [24] data set "F,11A,Ni200-CS", see Fig. 7.

The accuracy of experimental data were reported by Antonetti [18], Fisher [24], and Hegazy [19] to be 8.1, 5, and 7 percent, respectively. Unfortunately, the uncertainty of other researchers data are not available. The present model shows good agreement over the entire range of the comparison with the experimental data, which cover a wide range of the input parameters, see Table 2. The data also include the contact between dissimilar metals such as Ni200-Ag and SS-CS. The surface slope $m$ have not been reported by Clausing and Chao [23], Kitscha [25], Fisher [24], and Mikic and Rohsenow [17] and were estimated using a correlation proposed by Lambert and Fletcher [6], $m = 0.076\sigma^{0.52}$, where $\sigma$ is in micrometer. Because of the above-mentioned approximation to account for unreported data, the accuracy of the model is difficult to assess. However, the RMS and the mean absolute difference between the model and data for the entire set of data are approximately 14.8% and 10.6%, respectively.

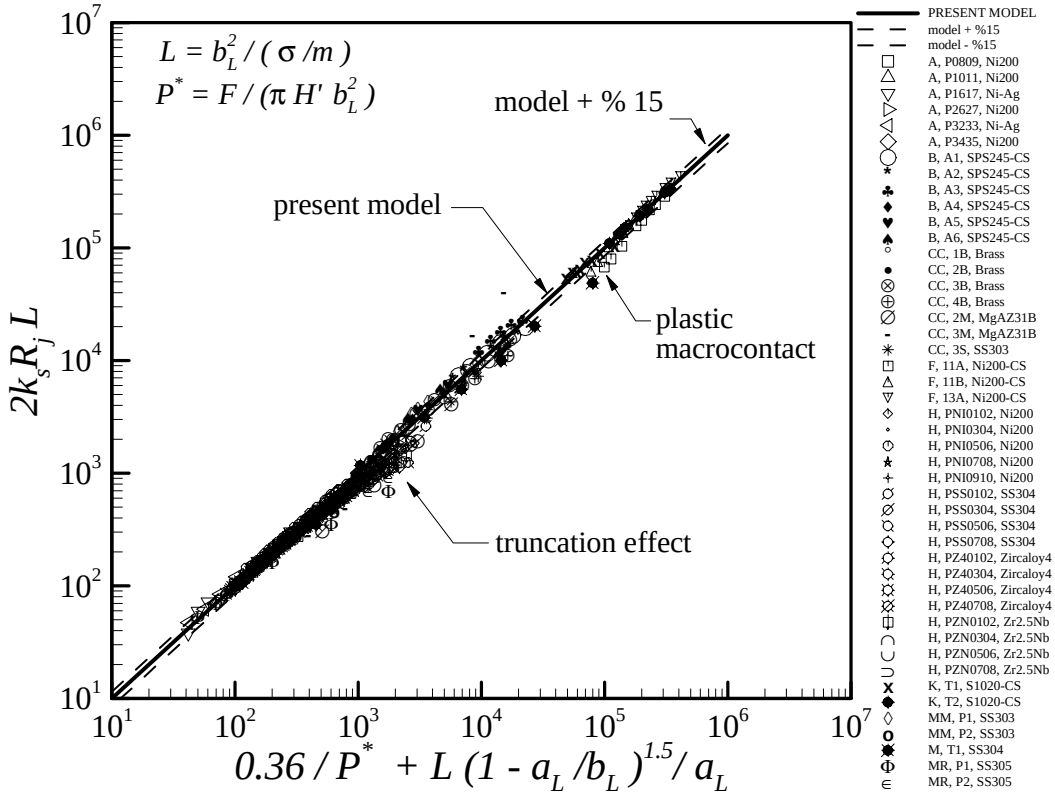


Figure 7. COMPARISON OF GENERAL MODEL WITH ALL DATA

Table 2. RANGES OF PARAMETERS FOR EXPERIMENTAL DATA

| Parameter |
|---|
| $7.15 \leq b_L \leq 14.28\ mm$ |
| $25.64 \leq E^{\theta} \leq 114.0\ GPa$ |
| $7.72 \leq F \leq 16763.9\ N$ |
| $16.6 \leq k_s \leq 227.2\ W/mK$ |
| $0.04 \leq m \leq 0.34$ |
| $0.12 \leq \sigma \leq 13.94\ \mu m$ |
| $0.0127 \leq \rho\ /\ 120\ m$ |

## 6 SUMMARY AND CONCLUSION

TCR of non-conforming rough surfaces was studied. It was shown that the joint resistance is the superposition of the macro and micro thermal resistances in a vacuum. Three regions were distinguished for TCR, the conforming rough limit, the elasto-constriction limit and the transition region.

It was shown that the heat source on a half-space assumption for the geometry of microcontacts is justifiable. In other words, microcontacts are located far (enough) from each other that they do not interfere and can be considered as heat sources on a half-space. Using scale analysis methods a new analytical TCR model was developed for the conforming rough contacts. In this study, instead of using probability relationships to calculate size and number of microcontacts, based on physical observations, for the first time scale relationships were derived. The scale relationships demonstrated the trends of the experimental data. The constant of the scale relationship was found through comparison with the data. This is a great example to demonstrate the power of "scale analysis" methods. In other words, it was shown that TCR can be determined without knowing the "exact" size and number of microcontacts.

The scale analysis relationship derived for the conforming rough contacts was integrated over the macrocontact area to extend the scale analysis model to cover the general contact or the transition region. An expression was derived for the effective micro thermal resistance of non-conforming rough contacts. Using the proposed correlation for the radius of the macrocontact by Bahrami et al. [21] and the

flux tube correlation the macro thermal resistance was determined. Superimposing the macro and the micro thermal resistances a general relationship for TCR was derived. This expression covers the entire TCR of rough contacts ranging from conforming to spherical smooth bare joints in a vacuum.

It was shown that the micro thermal resistance component of the joint resistance, $R_s$, is not a function of the surface curvature/out-of-flatness. Additionally, the profile of the effective contact pressure distribution did not affect the micro thermal resistance $R_s$.

The present model was compared with 604 TCR data points, which covered a wide range of surface characteristics, thermal and mechanical properties, and contact between dissimilar metals. The RMS difference between the model and data for the entire set of data is approximately 14.8% over the entire range of the comparison.

## ACKNOWLEDGMENT

The authors gratefully acknowledge the financial support of the Centre for Microelectronics Assembly and Packaging, CMAP and the Natural Sciences and Engineering Research Council of Canada, (NSERC).

## REFERENCES

[1] Bejan, A., Kraus, D., 2003, *Heat Transfer Handbook*, John Willey, New York.

[2] Tabor, D., 1952, *The Hardness of Metals*, Oxford, London.

[3] Greenwood, J. A. and Williamson, B. P., 1966, "Contact of Nominally Flat Surfaces," Proc., Roy. Soc., London A295, pp. 300-319.

[4] Bahrami, M., Culham, J. R., Yovanovich, M. M., and Schneider, G. E., 2003, "Review of Thermal Joint Models for Non-Conforming Rough Surfacces in a Vacuum," Paper No. HT2003-47051, ASME Heat Transfer Conference, July 21-23, Las Vegas Nevada.

[5] Clausing, A. M. and Chao, B. T., 1965, "Thermal Contact Resistance in a Vacuum Environment," Paper No.64-HT-16, Transactions of ASME: Journal of Heat Transfer, Vol. 87, November, pp. 243-251.

[6] Lambert, M. A. and Fletcher, L. S., (1997), "Thermal Contact Conductance of Spherical Rough Metals," Transactions of ASME, Vol.119, November, pp. 684-690.

[7] Nishino, K., Yamashita, S. and Torii, K., 1995, "Thermal Contact Conductance Under Low Applied Load in a Vacuum Environment," Experimental Thermal and Fluid Science, Elsevier, New York, 10, pp. 258-271.

[8] Johnson, K. L., 1985, *Contact Mechanics*, Cambridge University Press, Cambridge.

[9] Francois, R. V., 2001, "Statistical Analysis of Asperities on a Rough Surface," Wear 249, pp. 401-408.

[10] Cooper, M. G., Mikic, B. B. and Yovanovich, M. M., 1969, "Thermal Contact Conductance," Int. J. Heat Mass Transfer, Vol. 12, pp. 279-300.

[11] Carslaw, H. S. and Jaeger, J. C., 1959, Conduction of Heat in Solids, 2nd Edition. Oxford Press., London.

[12] Yovanovich M. M., Burde, S. S. and Thompson, C. C., 1976, "Thermal Constriction Resistance of Arbitrary Planar Contacts With Constant Flux," AIAA 11th Thermophysics Conference, San Diego, California, July 14-16, Paper No. 76-440, pp. 127-139.

[13] Yovanovich, M. M., and Hegazy, A., 1983,"An Accurate Universal Contact Conductance Correlation for Conforming Rough Surfaces with Different Micro-Hardness Profiles,"AIAA Paper No. 83-1434.

[14] Sridhar, M. R. and Yovanovich, M. M., 1996, "Emprical Method to Predict Vickers Microhardness," Wear, Vol. 193, pp. 91-98.

[15] Milanez, F. H., Yovanovich, M. M., and Culham, J. R., 2003, "Comparisons Between Plastic Contact Hradness Models and Experiments," Paper No. AIAA2003-0160, 41th AIAA Aerospace Meeting and Exhibit, Jan. 6-9, Reno, Nevada.

[16] Yovanovich, M. M., 1986, "Recent Developments In Thermal Contact, Gap and Joint Conductance Theories and Experiment," Eight International Heat Transfer Conference, San Francisco, CA, August 17-22, pp. 35-45.

[17] Mikic, B. B., Rohsenow, W. M., 1966, "Thermal Contact Conductance," Technical Report No. 4542-41, Dept. of Mech. Eng. MIT, Cambridge, Massachusetts, NASA Contract No. NGR 22-009-065, September.

[18] Antonetti, V. W., 1983, "On the Use of Metallic Coating to Enhance Thermal Contact Conductance," Ph.D. Thesis, Dept. of Mech. Eng., University of Waterloo, Waterloo, Canada.

[19] Hegazy, A. A., 1985, "Thermal Joint Conductance of Conforming Rough Surfaces: Effect of Surface Micro-Hardness Variation," Ph.D. Thesis, Dept. of Mech. Eng., University of Waterloo, Waterloo, Canada.

[20] Milanez, F. H., Yovanovich, M. M., and Mantelli, M. B. H., 2003, "Thermal Contact Conductance at Low Contact Pressures," Paper No. AIAA2003-3489, 36th AIAA Thermophysics Conference, June 23-26, Orlando, FL.

[21] Bahrami, M., Culham, J. R., Yovanovich, M. M., and Schneider, G. E., 2003, "Thermal Contact Resistance of Non-Conforming Rough Surfaces Part 1: Mechanical Model," Paper No. AIAA2003-4197, 36th AIAA Thermophysics Conference, June 23-26, Orlando, FL.

[22] Burde, S. S., 1977, "Thermal Contact Resistance Between Smooth Spheres and Rough Flats," Ph.D. Thesis, Dept. of Mech. Eng., University of Waterloo, Waterloo,

Canada.
[23] Clausing, A. M. and Chao, B. T., 1963, "Thermal Contact Resistance in a Vacuum Environment," University of Illinois, Urbana, Illinois, Report ME-TN-242-1, August.
[24] Fisher, N. J., 1985, "Analytical and Experimental Studies of the Thermal Contact Resistance of Sphere/Layered Flat Contacts," M.A.Sc. Thesis, Dept. of Mech. Eng., University of Waterloo, Waterloo, Canada.
[25] Kitscha, W., 1982, "Thermal Resistance of the Sphere-Flat Contact," M.A.Sc. Thesis, Dept. of Mech. Eng., University of Waterloo, Waterloo, Canada.
[26] McMillan, R. Jr. and Mikic, B. B., 1970, "Thermal Contact Resistance With Non-Uniform Interface Pressures," Technical Report No. DSR 72105-70, Dept. of Mech. Eng. MIT, Cambridge, Massachusetts, NASA Contract No. NGR 22-009-(477), November.